Implementation of an adaptive burst DQPSK receiver over shallow water acoustic channel

A. Falahati

Abstract: In an environment such as underwater channel where placing test equipments are difficult to handle, it is much practical to have hardware simulators to examine suitably designed transceivers (transmitter/receiver). The simulators of this kind will then allow researchers to observe their intentions and carry out repetitive tests to find suitable digital coding/decoding algorithms.
In this paper, a simplified shallow water digital data transmission system is first introduced. The transmission channel considered here is a stochastic DSP hardware model in which signal degradations leads to a severe distortion in phase and amplitude (fades) across the bandwidth of the received signal. A computer base-band channel model with frequency non-selective feature is derived by the authors [10-11]. This system was based on full-raised cosine channel modelling and proved to be the most suitable for vertical and short-range underwater communication cs dther), with a reflected path (specula component, when the acoustic hydrophone receives reflected signals from surface and bottom of the sea) and a random path (diffused component, when the acoustic hydrophone receives scattered signals from the volume of the sea). The model assumed perfect transmitter-receiver synchronization but utilized realistic channel time delays, and demonstrated the time-varying characteristics of an underwater acoustic channel observed in practice. In this paper, they are used to provide a full system simulation in order to design an adaptive receiver employing the most advanced digital signal processing techniques in hardware to predict realizable error performances.

Keywords: underwater channel modelling, adaptive receivers, hardware digital signal processing, advanced detection and estimation schemes.

1 Introduction

The increasing number of oil and gas fields, together with the rising cost and danger of repairing sub-sea structures around these fields, has led to the increasing employment of remotely operated vehicles (ROV's), which use umbilical cables for communication and control. With the great risk that these cables may become entangled, growing interest has centred on the possibility of using a through water communication scheme for the ROV, and for the remote recovery of data.

Fig. 1 shows a block diagram of a digital communication system with a coherent receiver, having an underwater channel as its transmission path. Depending on the data rate and the path lengths, the first-arrival symbols should be detected correctly. But after a delay as a result of multi-path propagated environment, echo streams also arrive, resulting in constructive and destructive interference (i.e. a flat fading response describing a frequency non-selective channel). The amplitude and phase of the received signal will then have a time varying characteristics and for relative movement between transmitter and the receiver, there will be a Doppler spread (i.e. slowly fading response) [1-6].

The basis for the short-range simulation model presented here is to represent the received signal as the resultant of three components. First is a steady direct-path component whose amplitude decreases with range and is added to the reflected path (second component) that is the result of reflection from either bottom or surface of the sea, and diffused path (third component) that comprises of a number of scattered components. The reception of third path depends on sea conditions and can increase with range and can eventually dominate the received signal (as the distance between transmitter and receiver is increased). Thus the mean value of a received signal may no longer be used as a measurement parameter on its own and that the amplitude distribution depends only on the average power in the random component [7-9]. But as the range or frequency increases, further multi-path processes are observed due to superposition of a number of time-delayed components arriving over different paths [Fig. 2].

The input signal is first differentially encoded by using four phase PSK modulation (DQPSK) at burst rate of 5Kb/s (4.8Kb/s for data and 200b/s for training sequences) for transmission through a hydrophone [6],[11]. By passing the four level-coded symbols through a low pass filter, the high frequency harmonics of each symbol are suppressed and the bandwidth is further reduced (Fig. 1). The filter is essentially a waveform shaper that produces a four-level shaped base-band waveform. It is this waveform that modulates the carrier waveform for transmission through the water[12-15].

To account for phase distortion at the receiver, an adaptive linear filter is inserted before the detection process (Fig.1) to adjust the overall sampled impulse response of the channel and filter to be a minimum phase sequence. The employment of such a filter should lead to further reduction in the complexity of any detection schemes [20-23]. To cancel the effect of severe amplitude distortion, a conventional non-linear equalizer may be employed [11,23].

Iranian Journal of Electrical & Electronic Engineering, 2005.
Paper first received 23th July 2002 and in revised from 19th July 2004.
A. Falahati is with the Department of Electrical Engineering, Iran University of Science and Technology, Narmak, Tehran 16844, Iran.

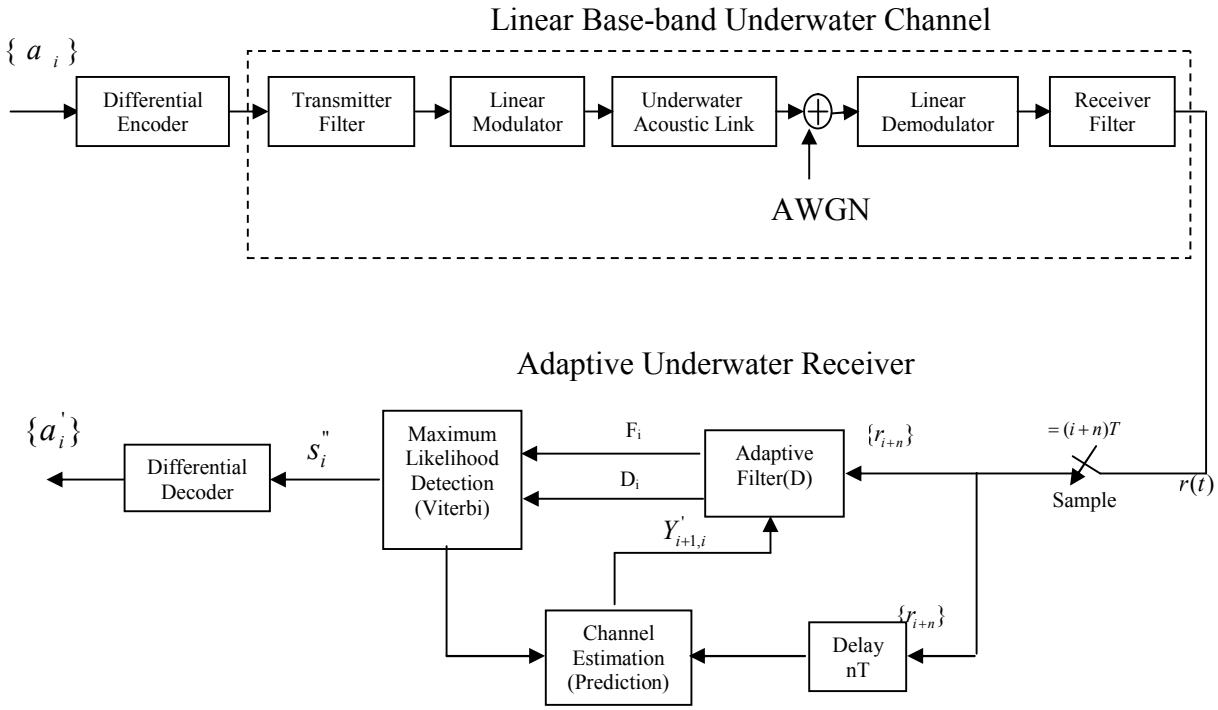

Fig. 1 An adaptive Digital data transmission system employing a shallow water channel model.

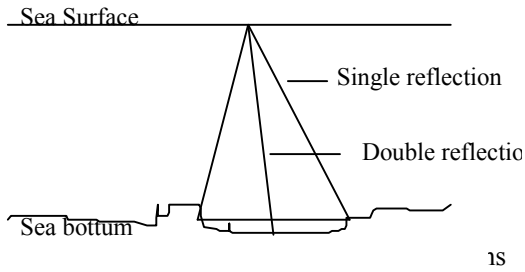

Fig. 2a Single and multiple specular reflections

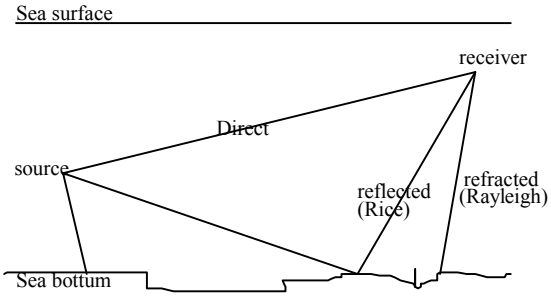

Fig. 2b Source andreceiver paths picture

Although this approach seems simple to implement, it requires a high signal level to extract information using a simple detector. But if the received sampled signal is followed by a vector detector that employs estimation process, a considerable improvement in tolerance to noise is achieved. However, the performance of both detectors fully depends on training sequences as well as the error signal produced for the adaptive adjustment of the sampled impulse response of the channel.

Finally, the short-range shallow underwater channel with Rayleigh together with a Rice statistics and the full transceiver system bearing an additive white Gaussian noise are implemented by hardware circuitry employing TMS320C5409-DSP devices functioning at 100MIPS (Million Instructions Per Second) to present overall system error performances [25-26]. Following statements amplifies the reasons why this particular device (TMS320C5409) is employed to produce the shallow water channel simulator and transceiver sections.

- Enhanced Harvard architecture built around one program bus, three data memory buses, and four address buses for increased performance and versatility.
- Advanced CPU designed with a high degree of parallelism and application-specific hardware logic for increased performance.
- A highly specialized instruction set for faster algorithms and for optimized high-level language operation.
- Modular architecture design for fast development of spin-off devices.
- Advanced IC processing technology for increased performance and low power consumption.
- Low power consumption and increased radiation hardness because of new static design techniques.

2 Digital implementation of shallow water channel model

Complete descriptions of a shallow water channel model fully described by the author previously [10-11] are available in the underwater literature, accounts for the channel with Rayleigh and Rice fading statistical distributions [1-11].

For digital implementation of the channel model (Fig. 3) it is neither practical nor necessary to represent the random fading sequences $V_i(t)$ as a continuous signal. These must be represented as discrete samples in time. However, $V_i(t)$'s have Gaussian spectra and hence theoretically they contain all frequency components.

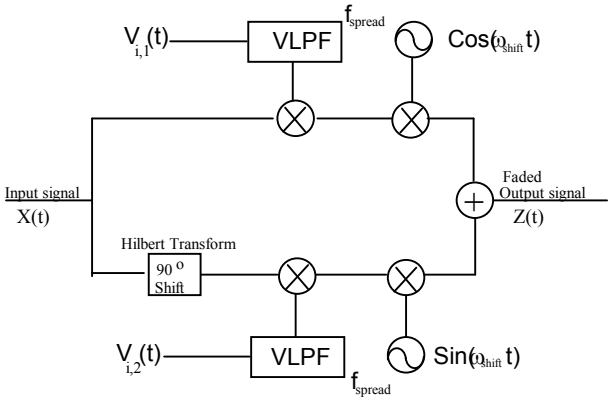

Fig. 3 Model of spectral spreading

For testing a 5Kb/s Differential Quadrature Phase Shift Keying (DQPSK) digital data modem over a short-range underwater channel with carrier frequency of 100KHz, it is necessary to use sampling rate of 2500-samples/second. It has been found that the impulse response and the magnitude-response of a Bessel filter tend towards Gaussian as the order of the filter is increased [7]. A Bessel filter has therefore, been used to obtain the necessary requirements in the design of the Variable Low-Pass Filters (VLPF) in the hardware simulation to produce one diffused component fading channel (Fig. 3). It is a combination of two 2-pole sections and a 1-pole section. The 1-pole section has a real pole whereas the 2-pole sections have complex conjugate poles. Thus when an un-modulated carrier with frequency f_c is transmitted, the equivalent low-pass received signal is:

$$r(t) = \sum_n \alpha_n(t) e^{-j\theta_n(t)} \tag{1}$$

Where

$$\theta_n(t) = 2\pi f_c \tau_n(t)$$

The received signal, at any given instant t, is thus the sum of a number of time-varying vectors having amplitudes $\alpha_n(t)$ and phases $\theta_n(t)$. Since $(1/f_c)$ is a small quantity, only a small change in $\tau_n(t)$ needed to change $\theta_n(t)$ by 2π radian. According to the random nature of underwater propagation, variations in $\tau_n(t)$ and $\theta(t)$ are also random. The fading is caused mainly by variation in the relative phases of the individual $\{\theta_n(t)\}$.

The next procedure is to convolute the transmitter and the receiver low-pass filters (shaping filters) with the produced Rayleigh and Rice channels. Design and implementation of root raised cosine filters is described elsewhere [10-11, 23]. It is confirmed that these equipment filters, a(t) and b(t), only introduce about 0.15dB amplitude distortion into the received signal amplitude but no phase distortion [22]. Thus, when overall convolution (transmitter filter, channel and receiver filter) is performed, vector $Y_i(t)$ is obtained by sampling $Y_i(t - iT)$ at a rate of 2500 samples per second. This vector then has h-complex sequence (with $h = 0,1,2,3,.....,g$) given by:

$$Y_i = y_0, y_1, ..., y_g \tag{2}$$

3 Realization of channel distortions

Consider the receiver of a practical underwater communication link with multi-path frequency non-selective fading characteristics. The highly distorted signal in phase and amplitude is sampled once per data symbol to establish a minimum phase response. The inter-symbol interference caused by phase distortion can be removed by means of a pre-filter ahead of a Viterbi detector [Fig. 1] with tap gains given by the roots of the polynomial of the estimated/predicted sampled impulse response of the channel with no reduction in tolerance to noise. But the amplitude distortion tends to reduce tolerance to noise of even the most optimum detector performing the maximum likelihood estimation process.

In order to represent the two distortions, consider the z-transform of the samples in (2) as:

$$Y_i(z) = y_{i,o} + y_{i,1} z^{-1} + y_{i,2} z^{-2} + ... + y_{i,g} z^{-g} \tag{3}$$

With the general form of:

$$Y(z) = y_o (1 - \gamma_1 z^{-1})(1 - \gamma_2 z^{-1})(1 - \gamma_g z^{-1}) \tag{4}$$

The distortions are then recognized by setting this expression to zero so that the values of z define the roots (zeros) of $Y(z)$.

In order for the polynomials to achieve full convergence, the roots must be as accurate as possible. Sequences of $Y(z)$ that do not lie within the unit circle can be forced to be minimum phased by including poles at the locations $z = \gamma_i$ where $|\gamma| > 1$ can cancel the effect of these zeros, and by adding new zeros at values of z given by the complex conjugates of their reciprocals of γ_i. This describes a phase transformation process on the sequences of Y_i.

The most effective method of ensuring such a phase transformation could be the employment of a linear pre-filter or an adaptive equalizer ahead of the detector, so that the channel and the linear filter together have a response that is a minimum phase [18-21]. This phenomenon can be accomplished by separating $Y(z)$ into two polynomials, one including those roots inside the unit circle plus the constant multiplication factor (amplitude distortion), and the other including roots outside the unit circle plus the delay (phase distortion). It is assumed that no roots of $Y(z)$ lie exactly on the unit circle in the z-plane:

$$Y(z) = Y_1(z) Y_2(z) \tag{5}$$

where:

$$Y_1(z) = \mu(1 + \alpha_1 z^{-1})(1 + \alpha_2 z^{-1})(1 + \alpha_{g-m} z^{-1}) \tag{6}$$

and:

$$Y_2(z) = z^{-m}(1 + \beta_1 z)(1 + \beta_2 z)(1 + \beta_m z) \tag{7}$$

where α_i is the negative of a root of $Y(z)$ and β_i is the negative of the reciprocal of a root of $Y(z)$, so that

$$|\alpha_i| < 1 \quad \text{and} \quad |\beta_i| < 1 \tag{8}$$

μ represents the appropriate complex value needed to satisfy (6) and (7). Now the sampled impulse response of the pre-filter can be approximately written as:

$$D(z) = z^{-m} Y_2^{-1}(z) Y_3(z) \tag{9}$$

where

$$Y_3(z) = (1 + \beta_1^* z^{-1})(1 + \beta_2^* z^{-1})(1 + \beta_m^* z^{-1}) \tag{10}$$

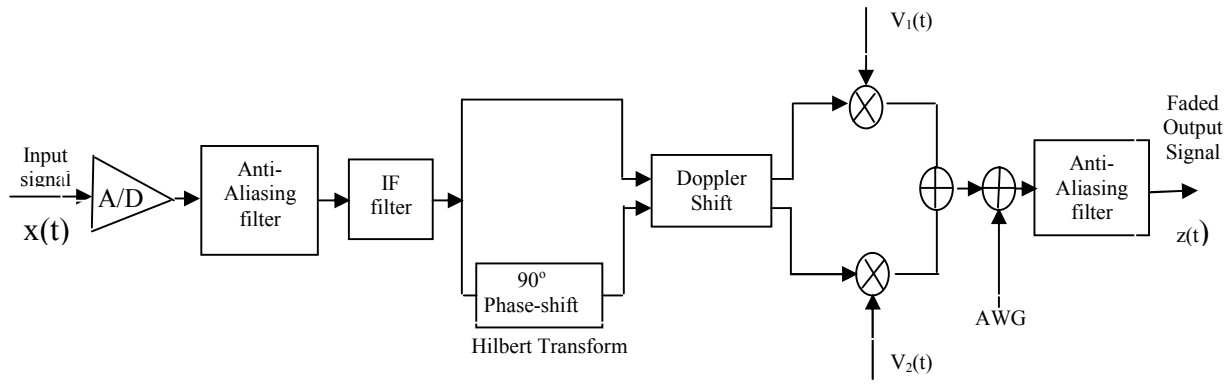

Fig. 4 One diffused component(with Doppler) hardware simulator.

and β_i^* is the complex conjugate of β_i Thus the z-transform of the channel and linear filter is approximately

$$F(z) = Y(z)D(z) = z^{-m}Y_1(z)Y_3(z) \qquad (11)$$

The accuracy of the system given by (8)-(11) can only be satisfied when $m \to \infty$, such a large value for m is unacceptable but a realizable m-tap filter can be produced by taking a good approximation.
It is now evident that all the roots of $F(z)$ lie inside the unit circle in the z-plane, thus satisfying the condition that the base-band channel, together with a linear pre-filter have a minimum phase response [19-20].
Furthermore, the roots of $Y_3(z)$ are the complex conjugates of the reciprocals of the roots of $Y_2(z)$, so that the linear filter replaces all roots of $Y(z)$ that lie outside the unit circle of $Y_2(z)$ by the complex conjugates of their reciprocals, leaving the remaining roots of $Y_1(z)$ unchanged. The linear filter achieves linear transformation on the received sequences of $\{r_i\}$ while keeping the level of data signal as well as the channel noise statistics unchanged [7].

4 Adaptive shallow water receiver employing detection and estimation techniques

A. Linear Adaptive Pre-detection Filter

The adaptive linear feed-forward transversal filter ahead of the detector shown in Fig. 1 is included in the system to minimize the phase of the received multi-path propagated sampled impulse response [21-22] of the determined short range shallow water channel with training sequences at 200b/s [Fig. 5].

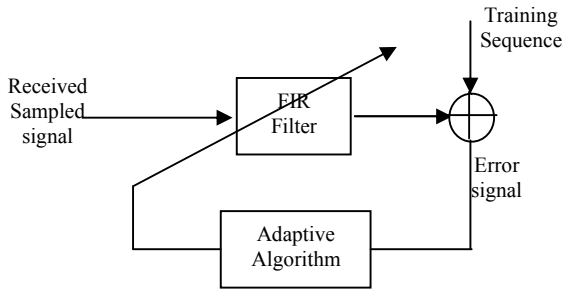

Fig. 5 Receiver employing adaptive algorithm

For a realistic practical system employing DSP hardware devices [24-25], consider this filter has a response given by:

$$D_i = [d_{i,0}d_{i,1}d_{i,2}...d_{i,n}] \qquad (12)$$

where n is the number of tap gains of the filter. The filter output r_i' upon the reception of r_{i+n} is then

$$r_i' = \sum_{k=0}^{n} r_{i+n-h}d_{i,k} \qquad (13)$$

This is further processed by the detector that operates on the estimated sampled impulse response of the cascaded channel and the filter given by:

$$F_i = [f_{i,0}f_{i,1}f_{i,2}...f_{i,n}] \qquad (14)$$

Determination of F_i takes place by the adaptive filter prior to the reception of r_{i+n}. The adjustment of the tap gains of D_i are obtained straight from the one-step prediction of the channel's sampled impulse response given by $\{Y'_{i+1,l}\}$.
The root finding algorithm fully explained in Refs. 21-23 is employed by the filter which functions in an iterative manner to obtain the zeros of $\{Y'_{i+1,l}\}$ in sequence. These roots are then used by the filter to asses the new tap gains of the adaptive filter D_{i+1} as well as forming the new resultant sampled impulse response of the channel and the filter F_{i+1}. The prior knowledge of the channel becomes available to the root-finding system since it processes on the previously determined roots.
Employing section 2, the root finding procedure as performed by DSP device is briefly explained for the simulation purposes now that the estimated sampled impulse response of the channel is obtained The algorithm first sets F_i to the least one-step predicted sampled impulse responses $\{Y'_{i+1,l}\}$as well as setting the transfer function of D to z^{-n}. Then, the corresponding values of the already determined roots in the previous iteration are set for starting point λ_0 [Fig. 7a] after which the initial start-up values of 0, +0.909, +0.909j, 0.909/2(+1+j) were taken up [23].
The evaluation of each λ_0 value is indicated s follows:

jconv=0

* Repeat The Loop For Convergence

$$e_{jconv,h} = f_h - \lambda_{jconv}e_{jconv,h+1}$$

for $h = g, g-1,...,1,0$

$$e_{jconv,g+1} = 0$$

$$\varepsilon_{jconv} = \sum_{h=1}^{g} e_{jconv,h}\lambda_{jconv}^{h-1}$$

$$\lambda_{jconv+1} = \lambda_{jconv} + \frac{e_{jconv,0}}{\varepsilon_{jconv}}$$

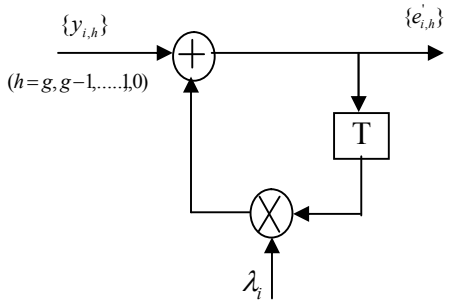

a) One tap feedback filter

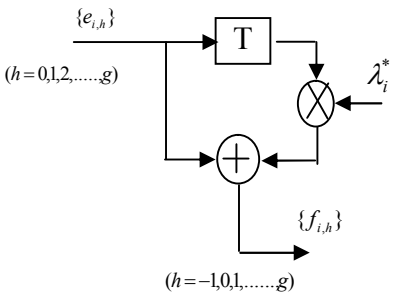

b) Two tap feed-forward filter

Fig. 6 One and two tap filters employed by pre-detection process

$\text{jconv} = \text{jconv} + 1$

IF $\left|\frac{e_{\text{jconv},0}}{\varepsilon_{\text{jconv}}}\right|^2 < d$

ORELSE satisfy any of jconv>50 & $|\lambda_{\text{jconv}}|>1$ & $\varepsilon_{\text{jconv}} \to 0$

TERMINATE (the iteration process is taken to be diverged)

THEN (proceed to the next possible value of λ_0)

IF (a root is located with the IF condition *THEN* store λ_k for the next iteration)

THEN (new values for F and D are determined as follows)

$f_h = f_{k,h+1} + \lambda_k^* e_{k,h}$ for $h = -1,0,1,.....,g$, $e_{k,-1} = 0$ where $f_{-1} = e_{k,0} = 0$

and $e_h = d_h - \lambda_k e_{h+1}$ for $h = n, n-1,.....,1,0$, $e_{n+1} = 0$

$d_h = d_{h+1} + \lambda_k^* e_h$ for $h = -1,0,1,.....,n$, $(e_{-1} = 0)$

where $d_{-1} = e_0 = 0$

with the one and two tap filters described in Fig. 6.

Using the updated values of F and D, the procedure is repeated with new values of λ_0.

ENDIF all the previous located roots have been assigned and all the nine start-up values of λ_0 have been tried out and no roots have been located[24].

The root-finding algorithm that was obtained "off-line" in [11,23] since it was considered as fully independent on any other parts of the systems in the receiver box. For a slowly time-varying channel that is implemented here with a powerful DSP processor, this algorithm can be performed in real time. As will be described in hardware section, the transmitter and receiver transducers are first considered to be almost stationary, the procedure is carried out once for every four or six samples or so but as the system starts to move, fewer samples are taken, at the expense of higher DSP board storage and processing time [25,26].

B. Channel estimation and echo cancellation techniques

The data detector of a sophisticated receiver of Fig. 1 extract the correct data by estimating (if necessary, predicting) the variation in the sampled impulse response of the channel. These sampled impulse responses could now include echoes present in the channel and can be identified by the channel estimator for removal by the detector, which regards them as inter-symbol interference [15-16,24].

Consider the channel estimator shown in Fig. 7. The system is essentially a linear feed-forward transversal filter. Each square T is a storing device holding the corresponding detected data symbol s'_{i-h}. On receipt of r_i, each time the stores are triggered, the stored values are shifted one place to the right. The detected data symbols $s'_i, s'_{i-1}, s'_{i-2}, ..., s'_{i-g}$ are then held in store following the detection of s_i. Each data symbol s_{i-h} is multiplied by the corresponding component $y_{i-1,h}$ of the estimate y_{i-1} of the vector Y_{i-1}, then their products are assumed to produce the estimate r_i of the received sample r_i as:

$$r'_i = \sum_h s'_i y_{i-h} \tag{15}$$

The error signal e_i is then obtained by subtracting (15) from the received signal r_i which is already held in store, i.e.

$$e_i = r_i - r'_i \tag{16}$$

The error signal e_i is then multiplied by a small positive real quantity 'b' to give be_i, which multiplies the complex conjugate $(s'_{i-h})^*$ of each detected data symbol s'_{i-h}. This product is then added to the corresponding components of Y'_{i-1} to produce the new stored estimate Y'_i as shown in Fig. 7. This implies the $(h+1)^{th}$ component of Y'_i given as:

$$y'_{i,h} = y'_{i-1,h} + be_i (s'_{i-h})^* \text{ for } h = 0,1,2,3,.....,g \tag{17}$$

The smaller the value of the parameter 'b', the smaller becomes the effect of additive noise on Y'_i but the slower the rate of response of Y'_i to changes in Y_i.

In the detection of s_i with a delay of n-1 sampling intervals (i.e. s_i is detected after the reception of r_{i+n-1}) the estimate of Y_i is only accessible on receipt of r_{i+n} for the detection of s_{i+1} so that the delay in estimation is the n sampling interval. Obviously, for the generation of error signals $e_i, e_{i+1}, e_{i+2}, ..., e_{i++n-1}$, the received samples $r_i, r_{i+1}, r_{i+2}, ..., r_{i++n-1}$ must be stored in a shift register. The error in using Y_i becomes excessive if the delay n or the number of the sampled impulse responses is large. The prediction $Y'_{i+n,1}$ of Y_{i+n} from the estimates of $Y'_i, Y'_{i+1}, ...$ then becomes necessary and the accuracy of the prediction is determined by the square of the error in $Y'_{i+n,i}$ as:

$$|Y_{i+n} - Y'_{i+n,i}|^2 = \sum_{h=0}^{g} |y_{i+n,h} - y'_{i+n,i,h}|^2 \tag{18}$$

The mean square error in $Y'_{i+n,i}$ is thus the average value of the squared error given in (18) over k transmitted symbols as

$$\xi = 10\log_{10}\left[\frac{1}{k}\sum_{j=1}^{k} |(y_{i+n})_j - (y'_{i+n,i})_j|^2\right] \tag{19}$$

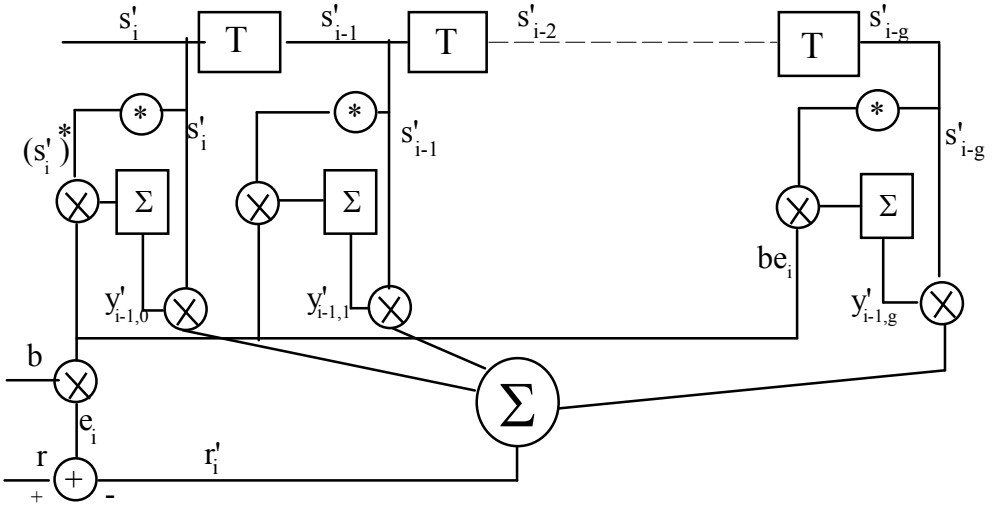

Fig. 7 Complex linear feed-forward estimator with degree zero prediction

This process (zero degree prediction) is probably the least complex form of estimation and involves relatively few operations per iteration. However, the first degree least-mean-square fading memory prediction operates the same way as above except that the updating equation $Y'_{i,i-1} = Y'_{i-1}$, for a channel amplitude that is slowly varying in time, is now replaced by the three following equations.

$$\phi_i = Y'_i - Y'_{i,i-1} \tag{20}$$

$$Y''_{i+1,i} = Y''_{i,i-1} + (1-\vartheta)^2 \phi_i \tag{21}$$

$$Y'_{i+1,i} = Y'_{i,i-1} + Y''_{i+1,i} + (1-\vartheta^2)\phi_i \tag{22}$$

where $Y'_{i,i-1}$ is the one step prediction given by (23)

$$Y'_{i,i-1} = [y'_{i,i-1,0}, y'_{i,i-1,1}, ..., y'_{i,i-1,g}] \tag{23}$$

to form the updated estimate of Y'_i which is the estimate of Y_i explained above by

$$Y'_i = [y'_{i,0}, y'_{i,1}, ..., y'_{i,g}] \tag{24}$$

and $Y''_{i,i-1}$ is a $(g+1)$-component row vector. The vector $Y'_{i+1,i}$ is the first degree least-mean square fading memory prediction of Y_{i+1}, and $Y''_{i+1,i}$ is the prediction of the rate of change with i of Y_{i+1}. The parameter 'ϑ" is a real-valued constant in the range 0 to 1, usually close to 1. .At the start of estimation process, $Y''_{0,-1} = 0$ and $Y'_{0,-1} = Y'_{-1}$, where Y'_{-1} is determined from setting this vector to the actual received sampled impulse responses or an appropriate training signal preceding transmission of data. It has been observed by many researchers [15,20-24] that the specific degree of the polynomial that results in the least mean square error may not produce the same mean square error on a different channel employing the same degree of prediction .

A. Reduced state Viterbi algorithm detector

The signal at the output of the filter D (Fig. 1), at time $t = iT$ is:

$$p_i = \sum_{h=0}^{g} s_{i-h} e_{i,h} + u_i \tag{25}$$

Transmission takes place by the n-level data-symbol $[s_i]$. The detector having a large storage capacity so that it can hold in store k ($k = n^g$) l-component vectors (sequences) $\{q_{i-1}\}$ before the reception of the signal p_i from the transversal filter D, where

$$q_{i-1} = [x_{i-1} x_{i-l+1} ..... x_{i-1}] \tag{26}$$

x_{i-h} are taken on a possible value for s_{i-h} for $h = 0,1,2,3,....., l$, the k-vectors $\{q_{i-1}\}$ being all different, indicating that all possible sequence of values that could be given by the data symbols $s_{i-l} s_{i-l+1} s_{i-l+2} ... s_{i-1}$ represented by the vector q_{i-1}.

Further to the reception of the signal p_i at the output of the filter D at time $t = iT$, each stored vector q_{i-1} is expanded into $n(l+1)$ component vectors $\{p_i\}$ where:

$$p_i = [x_{i-1} x_{i-l+1} .... x_i] \tag{27}$$

In each group of n vectors $\{p_i\}$, derived from any one vector q_{i-1}, the first l - component are as in the original q_{i-1} and the last component x_i takes on its l- different possible values.

Now introducing a parameter c (vector cost) that is calculated for each of the resulting l- vectors $\{p_i\}$ as:

$$c_i = c_{i-1} + | f_i - \sum_{h=0}^{g} x_{i-h} e_{i,h} |^2 \tag{28}$$

The smaller the value of c_i, the more likely is the corresponding data sequence correct. The appropriate store value c_{i-1}, is given by:

$$c_{i-1} = \sum_{j=0}^{i-1} | p_j - \sum_{h=0}^{g} x_{j-h} e_{i,h} |^2 \tag{29}$$

where $x_i = 0$ for $i < 0$ and $i > 1$.

The detected value s_{i-l} of data symbol s_{i-1} is now taken as the value x_{i-1} in the vector p_i with the smaller cost. The detector then discards any vector q_i whose first component x_{i-1} differs from s_{i-l} and select k vectors having the smaller costs $\{c_i\}$ from the remaining vectors $\{p_i\}$ (including that from which s_{i-l} was detected). The first component of each of the k selected vectors $\{p_i\}$ is now dropped (without changing its cost) to give the corresponding vectors $\{q_i\}$, which are then

stored, together with the associated costs $\{c_i\}$, ready for the next detection process. Such a discarding method employed here to the vectors $\{p_i\}$ ensures that the k stored vectors $\{q_i\}$ are always different, provided only that they were different at the first detection process, which can be easily arranged [10-11,21-24].

The performance of such a detector depends solely on severity of the amplitude distortion in the received signal as well as the number of stored vectors k. The main weakness of this detection process is the number of operation involved for k searches through kl costs particularly when h is large (say 16 or more). This excessive number of operations that could rise exponentially with increase in h can be reduced considering the employment of pseudo-binary and pseudo-quaternary detection schemes [24].

5 DSP hardware implementations and results

Fig. 8 presents the hardware implementation of proposed shallow water transceiver with channel simulator employing eight TMS320-C5409s with DSP8 acting as a master controller for synchronization and other control signalling purposes.

DSP1 is employed to generate real-time random data bearing training sequences for two minutes at 5Kb/s transmission rate. This processor and associated circuit also perform Polar RZ line coding on the generated data to produce necessary burst pulses. The reason to employ this coding technique is to ease element synchronization and tuning the transmitter at the desired DC level (presence or absence), better error detection performance, etc. This task can ease the system operation further by avoiding an extra board for scrambling.

DSP2 board is then programmed to ease relative $\pm 90^{\circ}$ fast phase changes that is present in a shallow water fading channel by Gray coding first and then differential coding. This board before performing DQPSK modulation also convolutes the entering pulses with a shaping filter (raised cosine filtering) amplitude components to further improve their properties, for example their spectral efficiency and/or immunity to inter-symbol interference. The distinction between line coding and pulse shaping is not always easy to make, and in some cases, it might be argued, artificial. Here, however, the distinction is made if for no other reason than to subdivide our discussion of baseband transmission into manageable parts.

Execution of the actual underwater shallow water channel takes place by a single board containing DSP3 and DSP4 [Fig. 8] with the amplitude response shown in Figs. 9. This figure reveals the acoustic hardware baseband channel output when only impulses are transmitted through shallow water model. The received signal $r(t)$ now sampled at t=iT is given by:

$$r_i = \sum_{h=0}^{g} s_{i-h}\, y_{i,h} + w_i \qquad (33)$$

w_i represents added sampled Gaussian noise at the output of the transmission path.

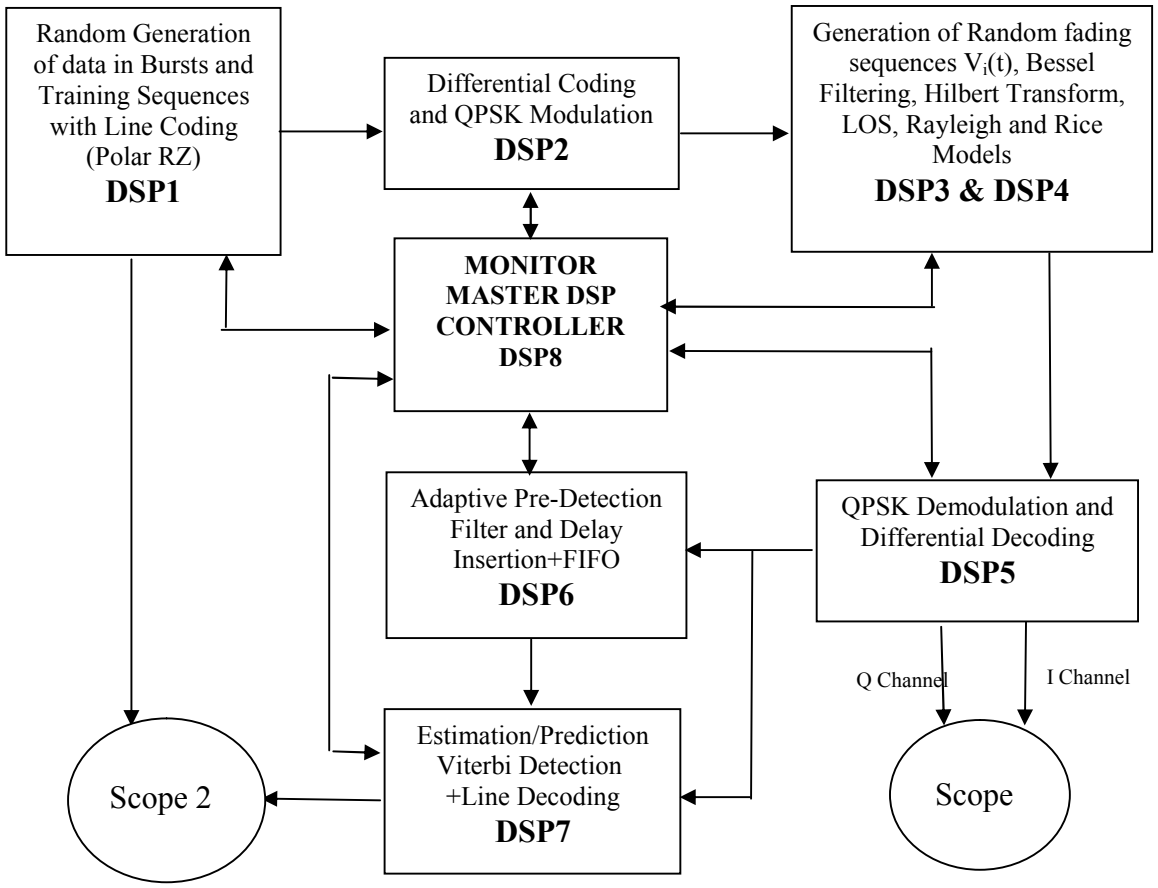

Fig. 8 Shallow water complete Modem employing DSP circuit boards.

Fig. 10 shows the channel's response with un-modulated carrier. This figure gives a true Rayleigh envelope for over 5 mili-second. of sample collections. The model performed here is a narrow-band sampling of the Bessel filter at 300Hz for ROV travelling at 0.8Knot.

Upon the reception of multi-path propagated DQPSK signals with observed fading, the receiver demodulates bursts that were passed through the hardware modulated base-band model [Section II] considering differential channel decoding with DSP5 board.

DSP6 digital signal processor board first inserts adequate delay of 18T (same number as received CIR) needed for the purposes of pre-detection matched filtering on the received un-modulated base-band signal. This processor then performs the adaptive pre-detection algorithm to obtain the minimum phase response.

At the heart of the receiver DSP7 performs the process of combined estimation/prediction and Viterbi detection algorithm. It is observed that after optimization of the prediction parameters the least mean square algorithm with degree one prediction provides a good mean square error performance. The received signal constellations diagrams with and without added noise is shown in Fig. 11.

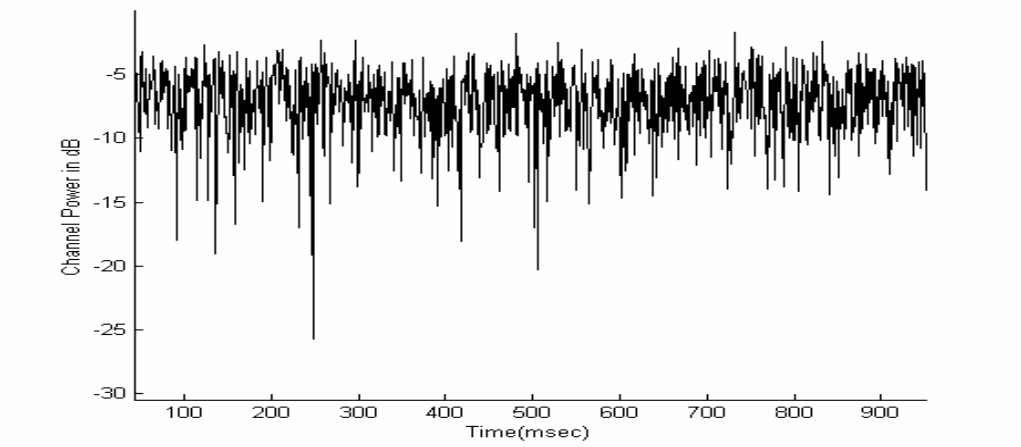

Fig. 9 Shallow water base-band channel amplitude fluctuation

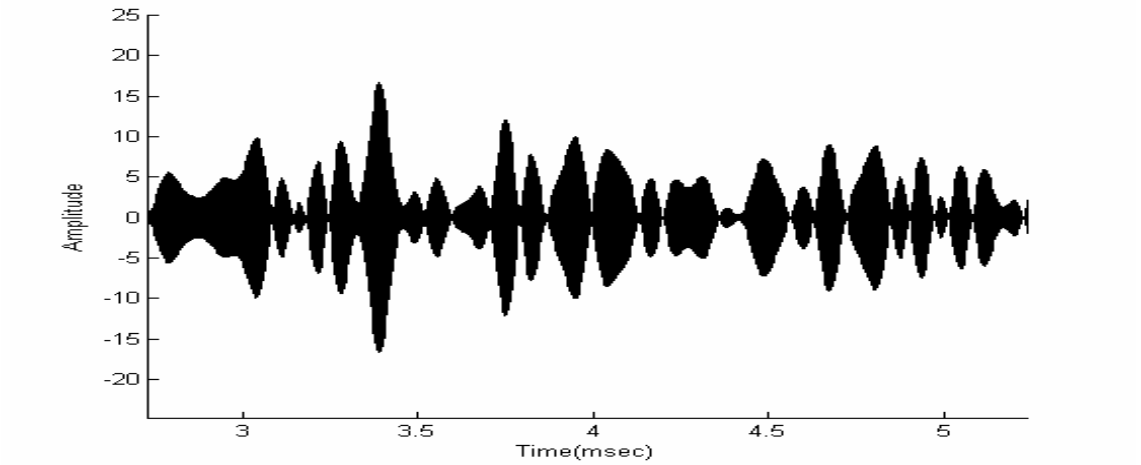

Fig. 10 hallow water spreading with un-modulated carrier (Rayleigh Envelope)

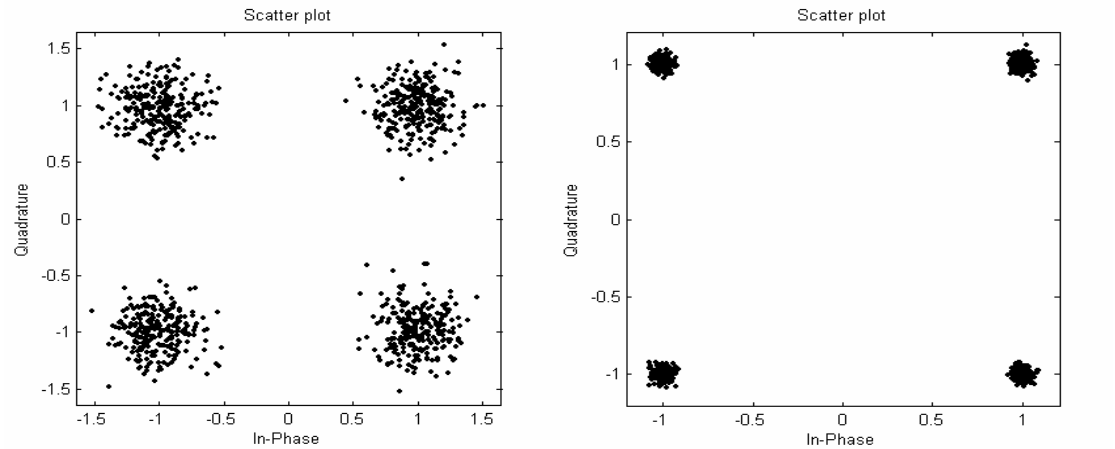

Fig. 11 Received signal constellations diagrams at the receiver input and after noise removal.

Fig. 12 indicates the error performance of the detector that can now be called the NML (Near Maximum Likelihood) detector since it does not employ all 18 samples but reduced to 11 valuable samples which are minimum phased. Thus Viterbi detector now employs the reduced CIR so that the processing time and storage are down to an acceptable value. Fig. 12 also indicates the performance of the receiver for different speed of the ROV, that of stationary, that of 0.2Knot (slow), 0.6Knot (moderate) and 0.8Knot fast.

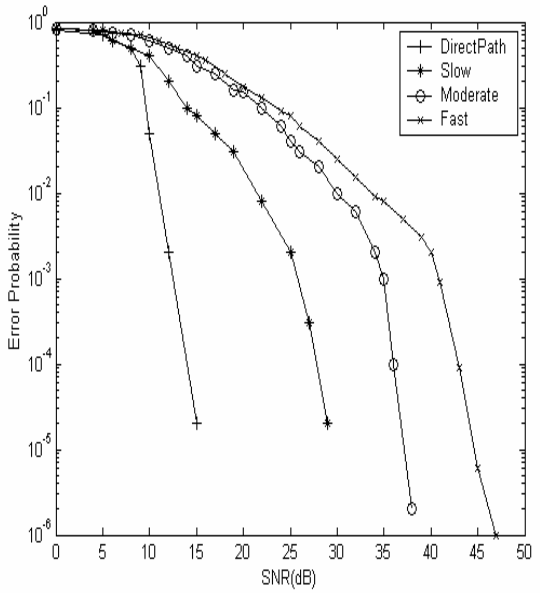

Fig. 12 Bit error rate performance of the full digital shallow water receiver at different speed of ROV.

6 Conclusion

The channel model presented here employs all non-linear characteristics that could be observed in a practical shallow sea conditions such as scattered and reflected paths, the ambient noise of the sea and possible echoes. The results shown here are produced by hardware boards and submitted to plotting software as data-files. Channel output gives clear indication of up to 30dB deep fades across the shallow water channel environment with a ROV travelling at moderately slow speed. The adaptive linear pre-detection filter ahead of combined estimator/detector not only provided a minimum phase response but also reduced the number of operations normally required for the Viterbi detector, that are a long processing time as well as a large storage capacity (production of a near maximum likelihood detector-NML). The application of such a detection technique although complex, not only provides a good error performances but also exhibit up to 3.5dB lower E_b/N_0 (or SNR) performance than that of any equalization technique. It should be emphasized that further reduction in tolerance to noise can be achieved by performing channel coding techniques. This subject too is under investigation to be implemented over the hardware simulator.

Furthermore, throughout this paper, the full system synchronization is performed by a special DSP board flag and the master controller (DSP8). But for the real system two further DSP boards need to be added to the system of Fig. 8 to perform the task of bit (in bursts) and carrier synchronization.

Looking through the hardware design of this sort, one can perform digital data communication algorithms in real-time with today's DSP technology a relatively easy practice. The hardware simulators of this sort can make the researchers think of difficult tasks the things of the past, perform many tests without going to the communication fields and still observe real and practical results. However, if a hardware simulated receiver of this kind can operate on channels with such a non-linear characteristics inserted in the model, it could well give a better performance over the actual channel.

8 References:

[1] C. Bjerrum-Niese and R. Lutzen, "Stochastic Simulation of Communication in Turbulent Shallow Water", IEEE J. Oceanic Eng. vol. OE-25, No. 4, pp523-532, Oct. 2000.

[2] R. Gavin and R. Coates, "A Stochastic Underwater Acoustic Channel Model", Proc. On Oceans 1996, Vol. 1, Fort Lauderdale. FL, pp. 203-210, 1996.

[3] M. J. Hinich, "A Statistical Theory of Signal Coherence", IEEE J. Oceanic Eng., Vol. 25, No. 2, pp 256-261, April 2000.

[4] J.G. Preising and M.P. Jhonson, "Signal Detection for the Underwater Acoustic Environment", IEEE J. Oceanic Eng., Vol. 26, No. 4, pp 572-585, Oct. 2001.

[5] A. Zielinski, Y. Yoon, and L. Wu, "Performance Analysis of digital acoustic communication in a shallow water channel", IEEE J. Oceanic Eng., Vol. 20, pp. 293-299, Oct. 1995.

[6] T.H. Eggen, J.C. Preisig, and A.B. Baggerover, "Communication Over Doppler Spread Channels-II: Receiver Characteristics and Practical Results", IEEE J. Oceanic Eng., Vol. 26, No. 4, pp. 612-621, Oct. 2001.

[7] A. Zielinski, R. Coates, L. Wang, A. Saleh, "High Rate Shallow Water Acoustic Communication" Proc. 93, Oceans, Vol.3, Victoria, BC, Canada, pp. 432-437, 1993.

[8] N. Cochard, J.L. Lacoume, P.Arzelies, and Y. Gabillet, "Underwater Acoustic Noise Measurement in Test Tanks", IEEE J. Oceanic Eng. Vol. 25, No. 4, pp 516-522, Oct. 2000.

[9] J.A. Capitovic, "Performance limitations in Underwater Acoustic Telemetry", IEEE J. Oceanic Eng. Vol. 15, July 1990.

[10] A. Falahati, B.Woodward, and S.C. Bateman "High speed digital data transmission over an underwater acoustic channel" Proc. Inst. Acoust., Vol. 9, pp. 4-15, Dec. 1987.

[11] A. Falahati, B.Woodward, and S.C. Bateman "Underwater acoustic channel models for 4800b/s QPSK signals" IEEE J. Oceanic Eng, Vol. OE16, No. 1, pp. 12-20, Jan. 1991.

[12] R.S. Andrews and L. F. Turner, "On the Performance of Underwater Data Transmission Systems Using Amplitude Shift Keying Techniques", IEEE Trans. On Sonics and Ultrosincs, Vol. SU-23, No. 1, pp 64-73, Jan. 1994.

[13] B. S. Sharif, J. Neasham and A. E. Adams "A Computationally Efficient Doppler Compensation

System for Underwater Acoustic Communications", IEEE J. Oceanic Eng. Vol. 25, No. 1, pp 52-61, Jan. 2000

[14] M. Badiey, Y. M. Jeffrey, A. Simon and S. E. Forsythe, "Signal Variability in Shallow-Water Sound Channel", IEEE J. Oceanic Eng. Vol. 25, No. 4, pp 492-500, Oct. 2000.

[15] J. G. Proakis, "Digital Communication" 2nd edn, McGraw-Hill, New York, 2000

[16] M. Stojanovic, J.A. Capitovic and J.G. Proakis, "Phase-Coherent Digital Communications for Underwater Acoustic Channels", IEEE J. Oceanic Eng. Vol. OE19, No. 1, Jan. 1994.

[17] P. M. Morse and U. Ingard, "Theoretical Acoustics", New York, McGraw Hill, 1968.

[18] W. C. Y. Lee, "Fundamental Design of mobile Communication", New York: McGraw- Hill 1995.

[19] G.S. Howe, O.R. Hintons, A.E. Adams and A.G. Holt, "Acoustic Burst Transmission of High Rate Data through Shallow Underwater Channels", IEE Trans. (Elec. Let.), Vol. 28, No. 5, Feb. 1992.

[20] J.G. Proakis, "Adaptive Equalization Techniques For Acoustic Telemetry Channels", IEEE J. Oceanic Eng., Vol. 16, No. 1, Jan. 1991.

[21] S. Haykin, "Adaptive Filter Theory", Englewood Cliffs, NJ, Prentice Hall, 1986.

[22] A.P. Clark, S. F. Hau, "Adaptive adjustment of a receiver for distorted digital signal", IEE Proc. F3, pp. 526-536, Aug. 1984.

[23] M. Jesuss, A. J. Silva, "Environmental Adaptive Equalizers in Underwater communications", Proc. Of MTS/IEEE Ocean'2004, Japan, April 2004..

[24] A.Falahati, "Channel models for underwater acoustic communications", PhD Thesis, Loughborough University of Technology, UK, 1992.

[25] Texas Instruments, "TMS320C54XX User's Guides", TI Publications Catalogues, 2000.

[26] Texas Instruments, "TMS320C54XX Application Manuals", TI Publications Catalogues, 2000.